

## FACILE SYNTHESIS OF HYDROXYAPATITE (HAp) NANOPARTICLES WITH DIFFERENT MORPHOLOGIES

D.C. Manatunga<sup>1</sup>, W. R. M. de Silva\*<sup>1</sup> and K. M. N. de Silva<sup>2</sup>

<sup>1</sup>Department of Chemistry, Faculty of Science, University of Colombo, Colombo, Sri Lanka. E-mail: danushi15@gmail.com

<sup>1</sup>Department of Chemistry, Faculty of Science, University of Colombo, Colombo, Sri Lanka. E-mail: rohini@chem.cmb.ac.lk

<sup>2</sup>Sri Lanka Institute of Nanotechnology, Nanotechnology & Science Park, Mahenwatte, Pitipana, Homagama, Sri Lanka. E-mail: nalinds@slintec.lk

### ABSTRACT

This study investigated the use of different synthetic approaches to obtain morphologically different HAp nanoparticles that can be used mainly in drug delivery. For this, simple Co-precipitation was applied under increased temperature conditions. Additionally microwave irradiation, metal doping and surfactant mediated synthesis were utilized. Characterization was carried out using X-Ray diffraction (XRD), Fourier transform infra-red (FT-IR) and Scanning electron microscopy (SEM). According to XRD most of the HAp nanoparticles are crystalline in nature, whereas the HAp nanoparticles synthesized using metal doping consists an amorphous nature. FT-IR spectra reveals that the surfactants are attracted to the HAp nanoparticle surface. SEM data showed the synthesis of nanoparticles using microwave irradiation, high temperature, surfactants and metal doping are coral shaped, rod shaped, granular shaped and square shaped respectively.

**Key words:** Hydroxyapatite, nanoparticles, drug carrier, physisorption, porous, morphologies, cetyltri methyl ammonium bromide, microwave irradiation

### 1. INTRODUCTION

Hydroxyapatite having the chemical formula of  $\text{Ca}_{10}(\text{PO}_4)_6(\text{OH})_2$  is an inorganic ceramic material which is similar to the natural bone and teeth [1,2]. Because of its biocompatibility, osteoconductivity and bioactivity [1,3] its use is much common in biological applications like drug delivery [4], gene delivery [2], bone tissue engineering etc. [3,5].

The designing of drug delivery systems for the controlled and continuous release of the drugs has been one of the major concerns. However it is generally accepted that in order to deliver the drugs to a predetermined location, it should either possess a porous structure [1] or the functional groups to attach with the drug [6]. Of these two methods the physisorption of the drugs to a porous/hollow HAp surface could be considered as beneficial due to the readiness of the drug at the site which avoids the risk of elimination by the reticuloendothelium system which is possible due to the presence of additional coatings in functionalized surfaces [7]. This could highlight the importance of having a desired morphology/architecture for the purpose of drug delivery [1, 4, 8]. HAp has been identified as a proper candidate due to its high binding affinity

towards various molecules [2], biocompatibility, non-toxicity and non-inflammatory responses [8]. In addition HAp can be synthesized with various morphologies which could ultimately lead to porous bodies [1, 4, 8]. Co-precipitation technique has been the basis in the preparation [1-5, 9]. And in many of the cases the resulting nanoparticles were highly crystalline and needle in shape [4, 9]. Some have involved in the creation of porous [1, 4]/hollow [8] which has utilized harsh conditions like calcination [1,4,8] or the use of polymer structures followed with the calcination [10] with lengthy procedures [8,10]. Use of cationic surfactant during the synthesis is another approach which has couples again to calcination at the end to get nanorods [5]. Scientists have also attempted to synthesize calcium deficient HAp by microwave irradiation which has ultimately coupled to calcination [11]. The resulting nanoparticles were in commonest needle shape [11]. Metal doping has been another interesting avenue to get calcium deficient HAp for controlled drug delivery [12]. But even in these cases the resulting nanoparticles were needle shaped and they have required very lengthy procedures for the synthesis [12].

Eventhough there is much data reported in the area of preparation of drug carriers from HAp, it

is very clear that most of them have utilized lengthy cumbersome procedures, calcination and the obtained nanoparticles were needle in shape [4, 9, 11]. Therefore this study has attempted to synthesize morphologically different nanoparticles by following facile greener approaches to pick the best out of them to be used in the purpose of drug delivery.

## 2. METHODOLOGY

### 2.1. Materials and methods

$\text{Ca}(\text{NO}_3)_2 \cdot 4\text{H}_2\text{O}$  (99%),  $(\text{NH}_4)_2\text{HPO}_4$  (99.9%), cetyltrimethyl ammonium bromide (CTAB, 99.9%),  $\text{Zn}(\text{NO}_3)_2$  (98%) and  $\text{NH}_4\text{OH}$  (25%) were purchased from Sigma Aldrich. All the reagents were used without further purification. Double distilled water was used for all the steps.

### 2.2. Synthesis of HAp at Increased Temperature ( $\text{M}_1$ )

Precursor solutions were heated separately at 50 °C and later  $(\text{NH}_4)_2\text{HPO}_4$  was added in dropwise to  $\text{Ca}^{2+}$  solution under vigorous stirring ( $\text{Ca}/\text{P} = 1.67$ ). The pH was adjusted to 10 and maintained for a specific period of time at the same temperature. At the end nanoparticles were isolated using centrifugation and washed using double distilled water. The product was dried at 200 °C for 2 hours.

### 2.3. Synthesis of HAp via Microwave Irradiation ( $\text{M}_2$ )

$(\text{NH}_4)_2\text{HPO}_4$  of pH= 10 was added in dropwise to the  $\text{Ca}^{2+}$  solution under vigorous stirring ( $\text{Ca}/\text{P} = 1.67$ ). Mixing was continued for 30 mins and milky suspension was centrifuged at 6000 rpm. The resulting pellet was washed and subjected to microwave digestion using a domestic oven operating at 2.5 GHz, 800W over 1.5 minutes.

### 2.4. Synthesis of HAp in the Presence of $\text{Zn}^{2+}$ ( $\text{M}_3$ )

40 % wt.  $\text{Zn}(\text{NO}_3)_2$  was mixed with the  $\text{Ca}^{2+}$  precursor solution and the pH was adjusted to 9.  $(\text{NH}_4)_2\text{HPO}_4$  was added in dropwise to the  $\text{Ca}^{2+}$ ,  $\text{Zn}^{2+}$  solution and the medium's pH was maintained at 9-10 providing vigorous stirring ( $\text{Ca}/\text{P} = 1.5$ ). It was continued over few hours and subjected to centrifugation and subsequent washing steps. The resulting pellet was dried at room temperature.

### 2.5. Synthesis of HAp in the Presence of CTAB

### ( $\text{M}_4$ )

CTAB was mixed with an aqueous suspension of  $(\text{NH}_4)_2\text{HPO}_4$  and it was added in dropwise in to the  $\text{Ca}^{2+}$  precursor solution and the pH was adjusted to 9. The milky suspension formed was vigorously stirred at 65 °C while maintaining the pH at the same. Then it was centrifuged and washed. The pellet was dried at room temperature.

As synthesized samples were characterized using X-Ray diffraction (Bruker D8 FOCUS X-ray diffractometer,  $\text{Cu K}\alpha$  ( $\lambda = 1.5418 \text{ \AA}$ ) x-ray radiation) over the range of 5°-80°, Fourier transform infra-red spectroscopy (FT-IR, Bruker Vertex 80) over the range of 400- 4000  $\text{cm}^{-1}$ , and Scanning electron microscopy using Scanning electron microscope (SEM- SU 6600 HITACHI) under an operating voltage of 5.0 - 15 kV.

## 3. RESULTS

### 3.1. Crystallinity of the HAp Nanoparticles

XRD spectra of HA powders resulted from different synthetic approaches are shown in Figure 1. In all the samples the diffraction peaks corresponded to the standard HAp except in the sample  $\text{M}_3$ , which has given rise to a broad spectrum displaying its amorphous nature [3,8,9]. Introduction of Zn during the synthesis has ended up with this lowered crystallinity [12]. However the treatment at higher temperatures has resulted in sharp peaks which indicated that the crystallinity is high with those nanoparticles [9].

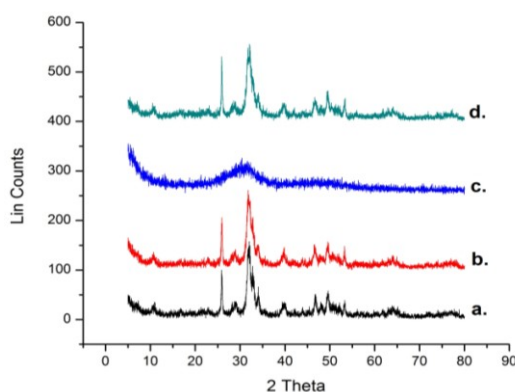
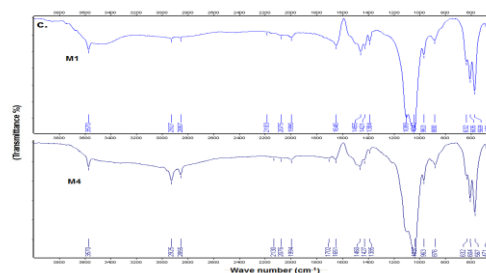
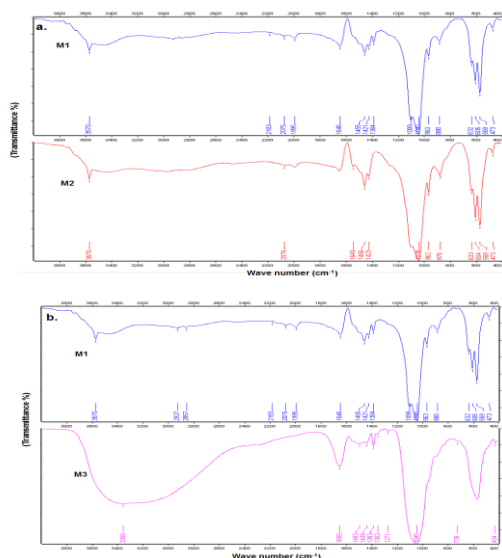


Figure 1: XRD spectra of resulting nanoparticles a.)  $\text{M}_1$ , b.)  $\text{M}_2$ , c.)  $\text{M}_3$ , d.)  $\text{M}_4$

### 3.2. FT-IR characterization

The FT-IR spectra for  $\text{M}_1$ ,  $\text{M}_2$ ,  $\text{M}_3$  and  $\text{M}_4$  are given in Fig.2. where  $\text{M}_2$ ,  $\text{M}_3$  and  $\text{M}_4$  have been compared with the  $\text{M}_1$ . All the samples have

demonstrated the characteristic HAp peaks [3, 9, 11]. The respective peaks of  $M_1$ ,  $M_2$  and  $M_4$  are much sharper and resolved than  $M_4$ . They displayed the obvious bands of HAp art around  $3570\text{ cm}^{-1}$  and  $632\text{ cm}^{-1}$  which are sharp and corresponding to  $-\text{OH}$  stretching and bending of HAp [3, 9, 11, 12]. Bands at  $1099\text{ cm}^{-1}$ ,  $963\text{ cm}^{-1}$ ,  $605\text{ cm}^{-1}$ ,  $473\text{ cm}^{-1}$  corresponds to  $\text{PO}_4^{3-}$  vibration of HAp in  $M_1$ ,  $M_2$  and  $M_4$ . But these bands are merged together and featureless in case of  $M_3$  which could be due to the low crystalline nature [12]. This is further proven by the presence of  $-\text{OH}$  band at  $3570\text{ cm}^{-1}$ ,  $632\text{ cm}^{-1}$  and  $\text{PO}_4^{3-}$  band at  $632\text{ cm}^{-1}$  with their intensities. The intensity of these bands can be taken as an indication of the crystallinity. Higher intense bands have given rise to more crystalline structure [9]. The corresponding intensities of  $M_1$ ,  $M_2$  and  $M_4$  are prominent than the  $M_3$  in this situation. In  $M_3$  sample there is a broad  $-\text{OH}$  stretching band in the region of  $3500\text{ cm}^{-1} - 2700\text{ cm}^{-1}$  which could be due to the presence of combined water [9]. This band is weaker in system  $M_1$ ,  $M_2$  and  $M_4$  which indicated that, higher the crystallinity lesser the content of combined water [9]. Additionally  $M_1$ ,  $M_2$  and  $M_4$  contained  $\text{CO}_3^{2-}$  peaks which could be due to the incorporation of  $\text{CO}_2$  during the preparation, which is much common [3,11]. In the case of  $M_4$  where the HAp has been synthesized in the presence of CTAB the respective bands that correspond to the two different CH band vibrations are also seen at  $2925\text{ cm}^{-1}$  and  $2855\text{ cm}^{-1}$  [13] in addition to the HAp major peaks.



**Figure 2:** FT-IR spectra of each system compared with  $M_1$  system a.)  $M_2$  compared with  $M_1$ , b.)  $M_3$  compared with  $M_1$  and c.)  $M_4$  compared with  $M_1$

### 3.3. Structure and Morphology of the Resulting Nanoparticles

SEM micrographs indicated that different morphological forms of HAp are formed when the reaction conditions are varied. As in Figure 3, when the reaction temperature is increased from the room temperature to  $50\text{ }^\circ\text{C}$  nanoparticles with an average length and a width of  $54\text{ nm}$  and  $21\text{ nm}$  with high homogeneity has formed. But the porosity of this sample was low as they were tightly arranged together. This morphology was different from the morphology in reported data at high temperature synthesis [9]. When the HAp nanoparticle suspension was subjected to microwave irradiation, a coral like inter connected nanoparticles with nanometer range cavities have formed. This was also different from the morphological forms that have been reported so far under microwave irradiation [11]. Moreover when metal doping was introduced square shaped nanoplates of  $60\text{--}70\text{ nm}$  size has formed. This morphology clearly shows the porous nature of the material formed. Apart from these, when a cationic surfactant like CTAB was introduced during the preparation of HAp, somewhat bigger granular shaped nanoparticles of average length and width of  $65\text{ nm}$  and  $29\text{ nm}$  has formed with a less porous structure.

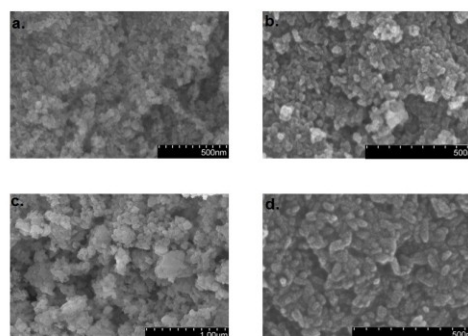


**Figure 3:** SEM micrographs of different systems a.)  $M_1$ , b.)  $M_2$ , c.)  $M_3$  and d.)  $M_4$

#### 4. CONCLUSION

From the above reported results it is very clear that the change or the variation of the reaction conditions could lead to a morphological variation in the resulting nanoparticles. More importantly this could help to pick the potential candidate for the purpose of drug delivery. It has been evidenced that the more porous structures have been much more interested in drug delivery [1,4]. Therefore the systems like M<sub>2</sub> which is having a coral like interconnected porous HAp scaffold will be suitable for this purpose. Additionally system like M<sub>3</sub> could also increase the adsorption and slow drug release due to its low crystalline nature [14]. More specifically in all these systems calcination, high temperature synthesis over a long period of time, aging has been avoided. As the experimental conditions are very simple, rapid and greener it highlights the possibility of synthesizing HAp nanoparticles in large scale.

#### 5. REFERENCES

- [1] Z. N. Al-Sokanee, A. A. H. Toabi, M. J. Al-assadi, and E. A. S. Alassadi, "The Drug Release Study of Ceftriaxone from Porous Hydroxyapatite Scaffolds", *AAPS PharmSciTech*, vol. 10, pp. 772-779, 2009.
- [2] S. H. Zhu, B. Y. Huang, K. C. Zhou, S. P. Huang, F. Liu, Y. M. Li, Z. G. Xue, and Z. G. Long, "Hydroxyapatite nanoparticles as a novel gene carrier", *Journal of Nanoparticle Research*, vol. 6, pp. 307-311, 2004.
- [3] B. Cangiz, Y. Gokce, N. Yildiz, Z. Aktas, and A. Calimli, "Synthesis and characterization of hydroxyapatite nanoparticles", *Colloids and Surfaces A: Physicochem. Eng. Aspects*, vol. 322, pp 29-33, 2008.
- [4] M. A. Martins, C. Santos, M. E. V. Costa, and M. M. Almeida, "Preparation of Porous Hydroxyapatite Particles to Be Used as Drug Delivery Systems", *Proceedings of Materials Science Forum*, pp 455-456, 2004.
- [5] J. M. Coelho, J. Agostinho Moreira, A. Almeida, and F. J. Monteiro, "Synthesis and characterization of HAp nanorods from a cationic surfactant template method", *Journal of Materials Science: Materials in Medicine*, vol. 21, pp. 2543-2549, 2010.
- [6] S. W. Choi, W. S. Kim, and J. H. Kim, "Surface-functionalized nanoparticles for controlled drug delivery", *Methods in Molecular Biology*, vol. 303, pp. 121-31, 2005.
- [7] F. Yu, and V. C. Yang, "Size-Tunable Synthesis of Stable Superparamagnetic Iron Oxide Nanoparticles for Potential Biomedical Applications", *Journal of Biomedical Materials Research A*, vol. 92, pp. 1468-1475, 2010.
- [8] P. Yang, Z. Quan, C. Li, X. Kang, H. Lian, and J. Lin, "Bioactive, luminescent and mesoporous europium-doped hydroxyapatite as a drug carrier", *Biomaterials*, vol. 29, pp. 4341-4347, 2008.
- [9] Y.X. Pang, and X. Bao, "Influence of temperature, ripening time and calcination on the morphology and crystallinity of hydroxyapatite nanoparticles", *Journal of the European Ceramic Society*, vol. 23, pp. 1697-1704, 2003.
- [10] L. Jiang, Y. Li, X. Wang, L. Zhang, J. Wen, and M. Gong, "Preparation and properties of nano-hydroxyapatite/chitosan/carboxymethyl cellulose composite scaffold", *Carbohydrate Polymers*, vol. 74, pp. 680-684, 2008.
- [11] A. Siddharhan, S. K. Seshadri, and T. S. S. Kumar, "Rapid Synthesis of Calcium Deficient Hydroxyapatite Nanoparticles by Microwave Irradiation", *Trends in Biomaterials and Artificial Organs*, vol. 18, pp. 110-113, 2005.
- [12] G. D. Vankatasubbu, S. Ramasamy, V. Ramakrishnan, and J. Kumar, "Nanocrystalline hydroxyapatite and zinc-doped hydroxyapatite as carrier material for controlled delivery of ciprofloxacin", *3 Biotech*, vol. 1, pp. 173-186, 2011.
- [13] K. Khoshnevisan, M. Barkhi, D. Zare, D. Davoodi, and M. Tabatabaei, "Preparation and Characterization of CTAB-Coated Fe<sub>3</sub>O<sub>4</sub> Nanoparticles", *Synthesis and Reactivity in Inorganic, Metal-Organic, and Nano-Metal Chemistry*, vol. 42, pp. 644-648, 2012.
- [14] A. Barroug, L. T. Kuhn, L. C. Gerstenfeld, and M.J. Glimcher, "Interactions of cisplatin with calcium phosphate nanoparticles: in vitro controlled adsorption and release", *Journal of Orthopaedic Research*, vol. 22, pp. 703-708, 2004.